



Spectral investigation of the Piperazine Dithiosemicarbazone Derivatives as inhibitor on High Carbon Steel in HCl media

R. Tamilarasan¹, A. Sreekanth^{1*}

1. Chemistry Department, National Institute of Technology Tiruchirappalli, Tiruchirappalli 620015 India.

Received 27 Jan 2017,

Revised 04 Aug 2017,

Accepted 10 Aug 2017

Keywords

- ✓ dithiosemicarbazone;
- ✓ high carbon steel;
- ✓ corrosion inhibition;
- ✓ electrochemical studies;
- ✓ FT-IR, XPS

Dr. A. Sreekanth
sreekanth@nitt.edu
+919489551851

Abstract

The inhibition efficiency of the piperazine dithiosemicarbazone derivatives on the corrosion of high carbon steel in HCL medium were studied by electrochemical impedance spectroscopy (EIS), polarization (Tafel), X-ray Photoelectron Spectroscopy (XPS) and UV-Visible spectroscopy. Electrochemical studies show that piperazine based dithiosemicarbazone derivatives acts as mixed type of inhibitors on high carbon steel. XPS data revealed that the inhibitors are adsorbed on the high carbon steel surface. It's also obeying the Langmuir's adsorption isotherm.

1. Introduction

Corrosion inhibitors were a classical way of protecting the materials against deterioration due to corrosion, especially in corrosive acidic media [1]. Organic compounds containing heteroatoms like O, N, and S are known to have superior inhibition qualities [2, 3]. In comparison to the large plethora of the organic inhibitors available, thiosemicarbazone derivatives have been reportedly more effective in acid medium corrosion due to the presence of the $-C=N$ and $-C=S$ groups in the molecule. Azomethane group have been widely reported as excellent inhibition of mild steel corrosion in the acidic medium due to the π electron donating ability. The nucleophilicity of the inhibitors evoked by π or lone pair of an electron on hetero atoms while binding with the electrophilic metal surface. Thiosemicarbazone has been investigated by several authors as effective corrosion inhibitors for mild steel. Several N- heterocyclic derivatives have been established to be a corrosion inhibitor in acidic medium. Thiosemicarbazone generally become effective by adsorption on the metal surface. The adsorbed species, protect the metal from aggressive medium, which causes decomposition of the metal. Adsorption not only the nature and charge of the metal, but on the chemical structure of the inhibitor [4-6, 46-47].

The aim of the present study to investigate the inhibiting properties of the Bis (pyridine-2-carboxaldehyde) piperazine dithiosemicarbazone (C1) and Bis (Benzoylpyridine) piperazine dithiosemicarbazone (C2) in the acidic medium. Mostly thiosemicarbazone derivative has been reported as protective in acidic medium, dithiosemicarbazone have a two $-C=N$ and $-C=S$ groups in the molecule and binding ability with steel more to reduce the corrosion. The inhibition efficiency of the inhibitor on the high carbon steel in 1M HCl was studied by means Electrochemical impedance spectroscopy, Tafel curve X-ray photoelectron, UV-Visible and Infra-Red spectroscopy and adsorption isotherm parameters are discussed.

2. Experimental details

2.1. Preparation of Bis(pyridine-2-carboxaldehyde) piperazine dithiosemicarbazone (C1)

1mmol of piperazine dithiosemicarbazone was dissolved in 20 ml of ethanol and 2 mmol of the pyridine 2-carbaldehyde was added to the solution and refluxed for 4 hours. A Yellow colored precipitate formed was then filtered, washed with ethanol and ether dried in a vacuum. Soluble in DMSO (Pale yellow) Yield: 85 %, M.P.

185⁰ C, Anal. Calc. for C₁₃H₁₄N₄O₂S₁: C, 52.41; H, 4.89; N, 27.16; S, 15.55. Found: C, 52.38; H, 5.82; N, 27.90; S, 15.53 %. IR data (KBr, cm⁻¹) 3441 (N-H), 1572 (C=N), 1294 (C=S). ¹H-NMR (500 MHz DMSO-D₆ ppm) 4.3 (8H, s, CH₂), 6.50 (2H, t, Ar), 6.57 (2H, d, Ar), 7.69 (2H, d, Ar), 8.69 (2H, d, Ar), 12.1 (1H, s, NH). ¹³C-NMR (125 MHz, DMSO-D₆, ppm):174.35 (1C, C=S), 166.35 (1C, C=N), 151.11, 112.00, 111.94, 111.10 (4C, Ar), 44.33(1C, CH₂).

2.2 Synthesis of Bis (Benzoyl pyridine) piperazinedithiosemicarbazone (C2)

1mmol of piperazine dithiosemicarbazone was dissolved in 20 ml of ethanol and 2 mmol of the Benzoyl pyridine was added to the solution and refluxed for 4 hours. A Yellow precipitate formed was then filtered and washed with ethanol and ether dried in a vacuum. Soluble in DMSO(Pale yellow) Yield: 88 %, M.P. 194⁰ C, Anal. Calc. for C₃₀H₂₈N₈S₂: C, 63.80; H, 5.00; N, 19.84; S, 11.36. Found: C, 63.43; H, 4.91; N, 19.50; S, 11.23 %. IR data (KBr, cm⁻¹) 3441 (N-H), 1572 (C=N), 1294 (C=S). ¹H-NMR (500 MHz DMSO-D₆ ppm) 3.35 (8H, s, CH₂), 6.50 -7.42 (Ar), 12.30 (1H, s, NH). ¹³C-NMR (125 MHz, DMSO-D₆, ppm):182.58 (1C, C=S), 160.35 (1C, C=N), 124.27-149.90, (Ar), 46.76(1C, CH₂)

2.3 Characterization of C1 and C2

2.3.1 Spectroscopic methods

The UV-Visible absorption spectrum was measured in the SHIMADZU-UV-2101PC UV-Visible spectrophotometers in the DMSO solution. FT-IR spectrum performed in the Nicolet spectrometers using KBr pellet. The ¹H, ¹³C NMR spectra were recorded in the Bruker 500MHz in DMSO-d₆. ¹H and ¹³C chemical shift are reported in ppm Vs TMS. Electron spray ionization mass spectrum was measured in the THERMO-FINNIGAN LCQ ADVANTAGE MAX mass spectrometer.

2.3.2 Electrochemical analysis

The electrochemical investigations were carried out using conventional three electrode systems with a saturated calomel electrode as reference and platinum electrode, as counter electrode respectively. The polished high carbon steel (HCS) with an exposed surface area of 1cm² in the solution was used as the working electrode. The electrochemical impedance spectroscopy and polarization studies have been performed on the CH instruments. The EIS measurements were carried out in the frequency range of 1-10000 Hz with an amplitude of the 10mV at the open circuit potential. The polarization studies have been performed in the range of 850 to -150mV with a scan rate of 1mV/S [7-10].

2.3.3. XPS analysis

The high carbon steel samples were immersed in the 1M HCl solution in the absence and presence of inhibitor for 2h. X-ray Photoelectron Spectrum was measured on Kratos Axis-Ultra DLD model instrument. The sample was irradiated with Mg K α ray source and analyzed with the 1cm² surface of the HCS. The electron binding energy was counterbalanced for charging effects by reference to the C1s binding energy of surface carbon at 285.0eV [11-14].

3. Results and Discussion

3.1. Characterization of the inhibitor

The dithiosemicarbazone derivatives were synthesized and good yields as per the scheme as shown in Fig.1. The UV-Visible spectrum of C1 showing the two characteristic bands at 290 and 300 nm corresponds to the n- π^* and π - π^* transitions arising from the thiosemicarbazone moiety. C2 shows two bands at 260 and 280 nm respectively. IR spectra of the two compounds show N-H stretch at 3441(C1) and 3400(C2), C=N stretching at 1572(C1) and 1570(C2), and C=S stretching at 1294(C1) and 1270(C2) cm⁻¹ respectively. These bands are characteristics of the structure as shown in fig.1.

3.2. Electrochemical impedance spectroscopy

Fig 2 showed the Nyquist plots of the HCS in the absence and presence of the inhibitor in the 1M HCl medium. The impedance curves reveal depressed semicircle capacitive loop at the higher frequency, small inductive loop at low frequency [15-17]. The capacitive loop originates from the adsorption on the reaction surface and charge transfer resistance (R_{ct}) [18-21]. The concentration of inhibitor changes from 20-100ppm, the surface layer increases with increasing the diameter of the depressed semi-circle, charge transfer resistance increases and there is a decrease in the dielectric constant as inferred from the tables. In terms of the constant phase element (CPE) expressed as following equation:

$$Z_{CPE} = K^{-1} (j\omega)^{-n}$$

K is the CPE constant (in $\Omega^{-1} s^n \text{ cm}^{-2}$), $j = \sqrt{-1}$, ω is the angular frequency in rad s^{-1} ($\omega = 2\pi f$, f is the angular frequency in Hz).

Figure 1: synthesis scheme and Structure of the C1-C2

Fig.2 and table 1, 2, data clearly indicating that R_{ct} values are increased and the capacitance (C_{dl}) values decrease while increasing the concentration of the inhibitor [22-25]. The surface layer increase with the increasing concentration of the inhibitor and the percentage inhibition efficiency reached the maximum for the inhibitor up to 95.3(C1) and 96.1(C2) at the 100ppm concentration. The compound (C2) act as a better inhibition efficiency compared to (C1). The data fit with a circuit consisting of the constant single-phase element charges-metal surface and solution [26-27].

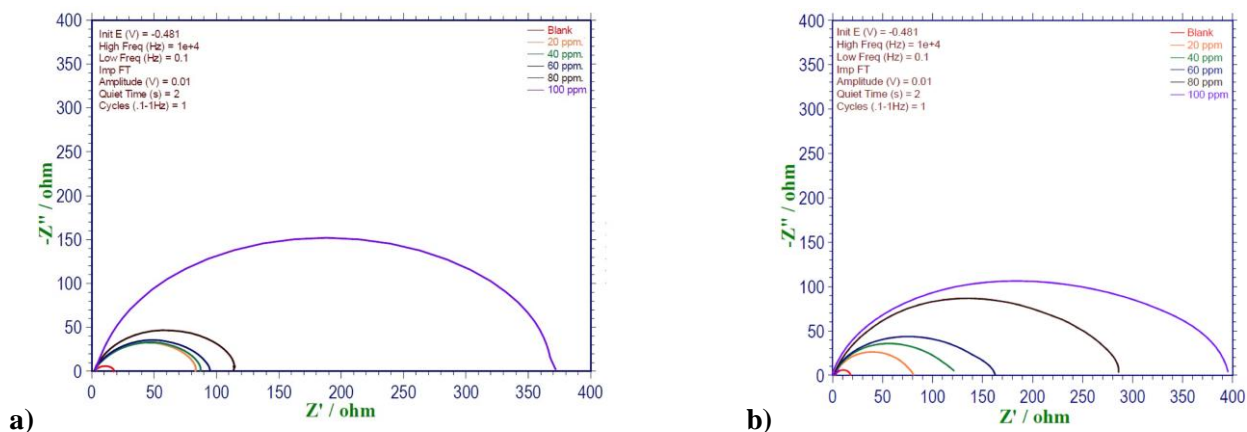


Figure 2: Electrochemical impedance spectra of HCS in 1M HCl in absence and presence of a) C1 b) C2

Table 1: EIS for HCS immersed in 1.0 M HCl solution in presence of various concentrations of C1.

Inhibitor concentration (ppm)	R_{ct} ($\Omega \text{ Cm}^2$)	C_{dl} ($\mu\text{F Cm}^2$)	IE (%)	θ
Blank	15.15	289.08		
20	81.2	97.22	77.8	0.778
40	120.0	41.87	85.8	0.850
60	162.2	37.55	88.9	0.889
80	292.0	30.63	93.8	0.938
100	395.0	10.33	95.4	0.954

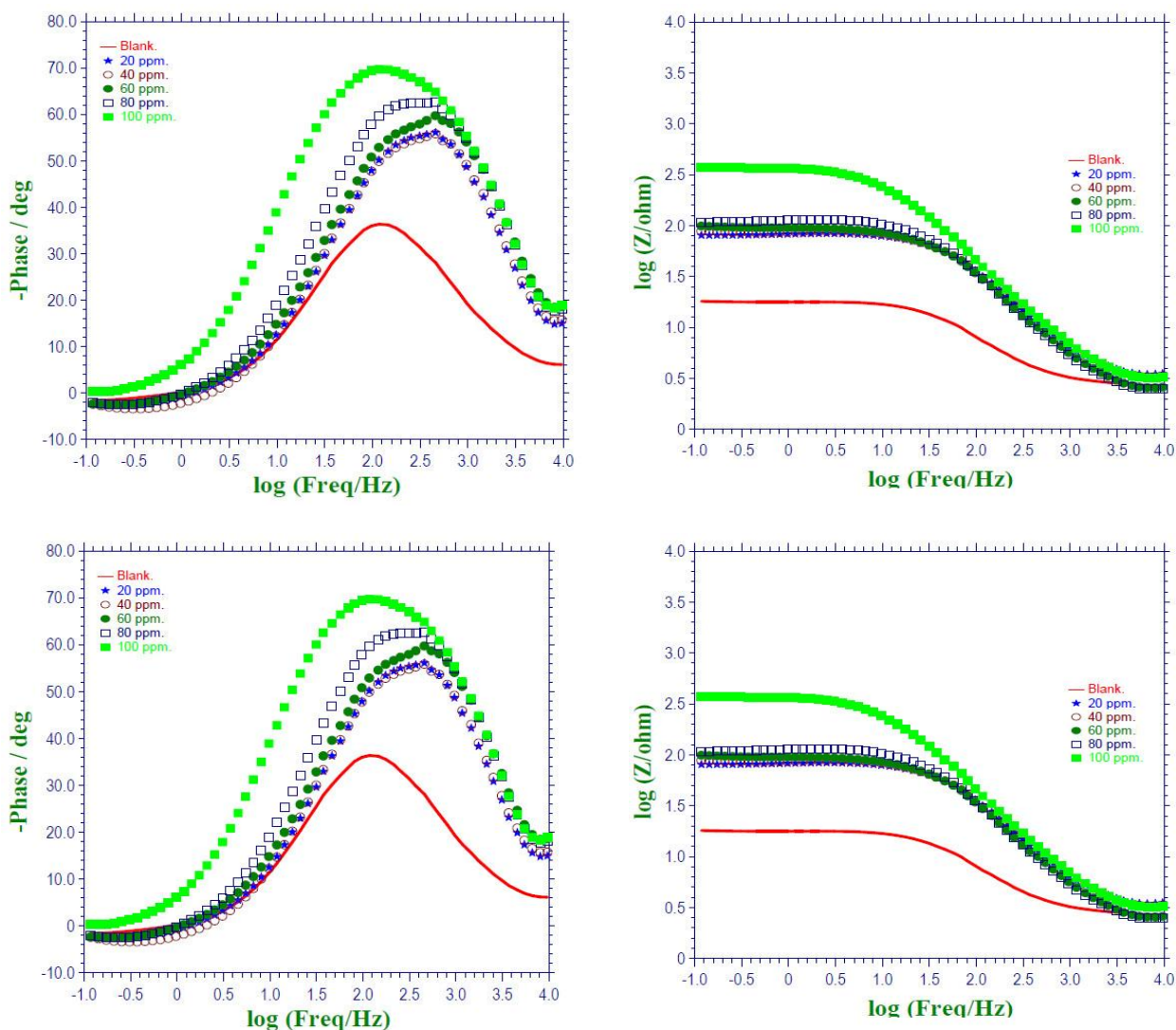


Figure 3: Electrochemical impedance spectra of HCS in 1M HCl in the absence and presence of a) C1 b) C2 Bode plot.

Table 2: EIS for HCS immersed in 1.0 M HCl solution in presence of various concentrations of C2.

Inhibitor concentration (ppm)	R_{ct} ($\Omega \text{ Cm}^2$)	C_{dl} ($\mu\text{F Cm}^2$)	IE (%)	θ
Blank	15.15	289.08		
20	81.5	35.85	80.9	0.809
40	121.7	23.13	87.2	0.872
60	162.9	15.92	90.5	0.905
80	286.2	8.74	94.6	0.946
100	395.5	4.17	96.1	0.961

3.3 Tafel polarization measurements

The results of the Tafel polarization measurements are shown in Fig 4. The electrochemical parameters such as corrosion potential (E_{corr}), corrosion current density (I_{corr}), anodic Tafel slope (b_a) and cathodic Tafel slope (b_c) were extrapolated from the curves are given in Table 3 for both the inhibitors. As seen from the Fig. 4. The adsorption of the inhibitor on the surface of the high carbon steel reduces the anodic dissolution of iron and delays cathodic hydrogen evolution reactions [28-32]. The corrosion potential does not shift remarkably while changing the inhibitor concentration. It clearly indicates that inhibitor acted as a mixed type of inhibitor in acid medium and C2 has better inhibitor efficiency than C1

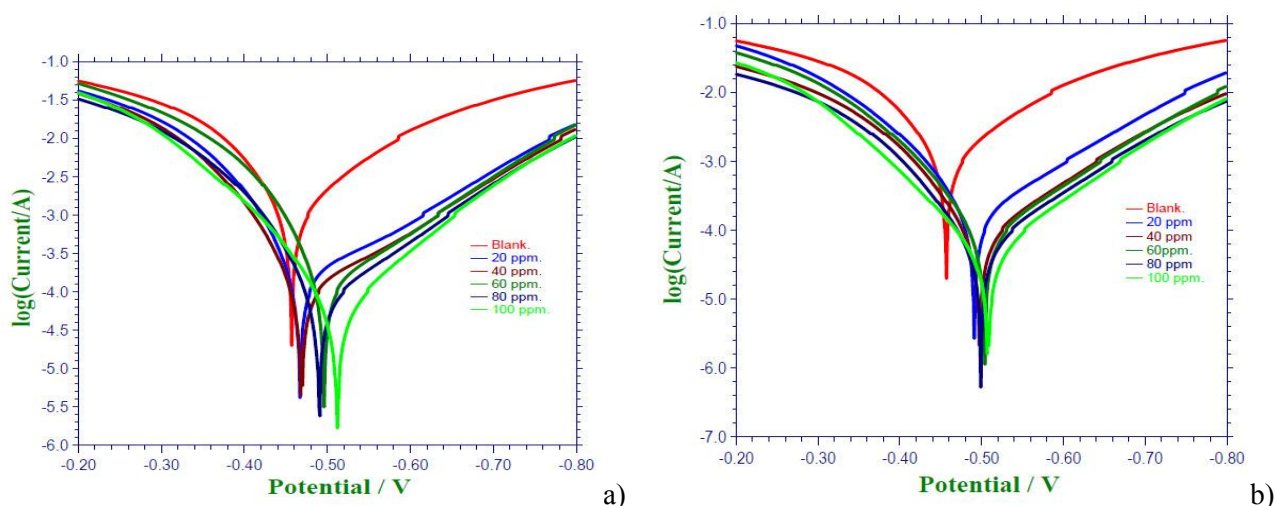


Figure 4: Tafel plots of HCS in 1M HCl in the absence and presence of a) C1 b) C2

Table 3: Tafel for HCS immersed in 1.0 M HCl solution in presence of various concentrations of C1.

Inhibitor concentration (ppm)	I_{corr} ($\mu\text{A cm}^{-2}$)	E_{corr} (V/SCE)	β_c (mV/dec ¹)	β_a (mV/dec ¹)	IE (%)	θ
Blank	15.01		7.304	8.471		
20	2.64	0.4720	6.23	7.105	82.42	0.82
40	1.94	0.4655	7.424	11.899	87.09	0.87
60	1.67	0.4733	5.589	9.531	88.94	0.89
80	1.15	0.4930	6.352	7.842	92.42	0.92
100	0.84	0.4890	6.230	7.105	94.40	0.94

Table 4: Tafel for HCS in 1.0 M HCl solution in presence of various concentrations of C2.

Inhibitor concentration (ppm)	I_{corr} ($\mu\text{A cm}^{-2}$)	E_{corr} (V/SCE)	β_c (mV/dec ¹)	β_a (mV/dec ¹)	IE (%)	θ
Blank	15.01		7.304	8.471		
20	1.72	0.4936	7.404	13.888	88.54	0.88
40	0.95	0.4969	6.734	11.770	93.67	0.93
60	0.87	0.5036	7.632	13.681	94.20	0.94
80	0.59	0.4956	7.643	12.654	96.10	0.96
100	0.48	0.5058	8.067	10.829	96.80	0.97

3.4 XPS spectrum of the C2

The XPS Spectrum measurement was carried out with the mechanically polished specimens of the high carbon steel in acid absence and presence of the inhibitor. The XPS core level spectra provide the valuable information about the chemical composition of inhibitor and the result shows in the (Fig 5). The C_{1s} spectrum of the inhibitor has been shown in Fig 5. The C_{1s} spectrum has the two kinds of the binding energy peaks at the 285.0 eV and 286.0 eV the first peak at 285.0 eV corresponds to the $-C-C-$ or CH_n binding energy peaks [33-34]. The second peak at 286.0 eV corresponds to the C-N of the inhibitor [37]. The N_{1s} spectrum has contained the number of overlapping spectrum, it has the peak at 400.0 eV corresponds to the C-N species, 401.0 eV related to the Fe-N species which nitrogen atom of the inhibitor interaction with the Fe atom in the high carbon steel [35-38]. The O_{1s} spectrum of the as shown in Fig 6., it comprises the overlapping of the number spectrum. Binding energy peak at 530.0 eV related to the OH species, the second peak at 531.2 eV related to the O^{2-} species [36-40]. The S_{2p} spectrum seen in Fig 6., it shows a single peak with several overlapping spectrums. The S_{2p} has the signal at the 162.0 eV due to the FeS, second signal at 164.0 eV due to the FeS_n . The Fe_{2p} spectrum have the three peaks, peak 711.0 eV correspond to the $Fe^{3/2}$ state, peak at 725.0 eV corresponds to the $Fe^{1/2}$, the third peak at 719.0 eV corresponds to the satellite peak of the inter system crossing of the $Fe^{3/2}$ and $Fe^{1/2}$ of the iron in the high carbon steel, in the case of the absence of the inhibitor on the high carbon steel there is no satellite peak it also further confirm that inhibitor has adsorbed on the surface of the high carbon steel and form the protective layer at the 100ppm concentration of the inhibitor[40-43]. The XPS results of the element of the C_{1s} , N_{1s} , O_{1s} ,

S_{2p} and Fe_{2p} reveals that inhibitor absorbed on the HCS surface and form the protecting layer which diminishes the corrosion.

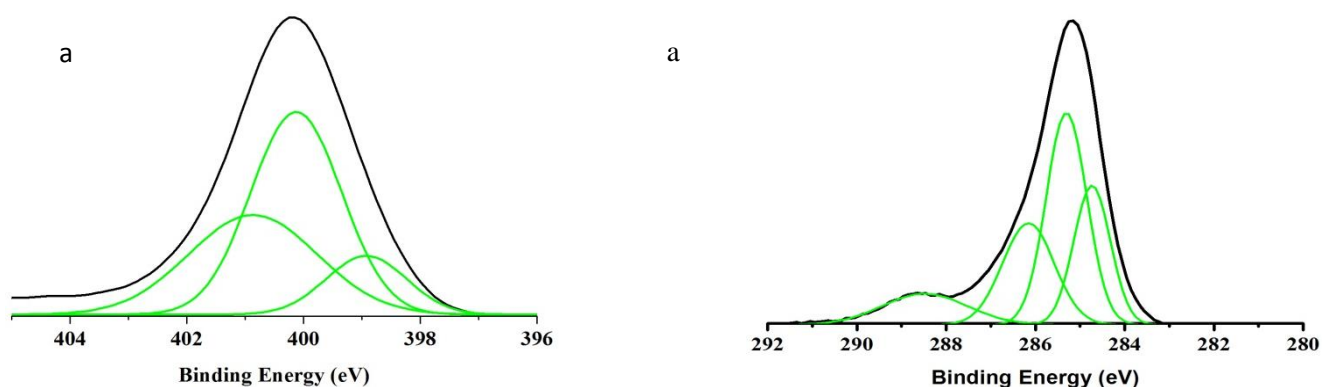


Figure 5: HCS spectra of a) N1s, b) C1s, in presence of 100ppm concentrations of C1

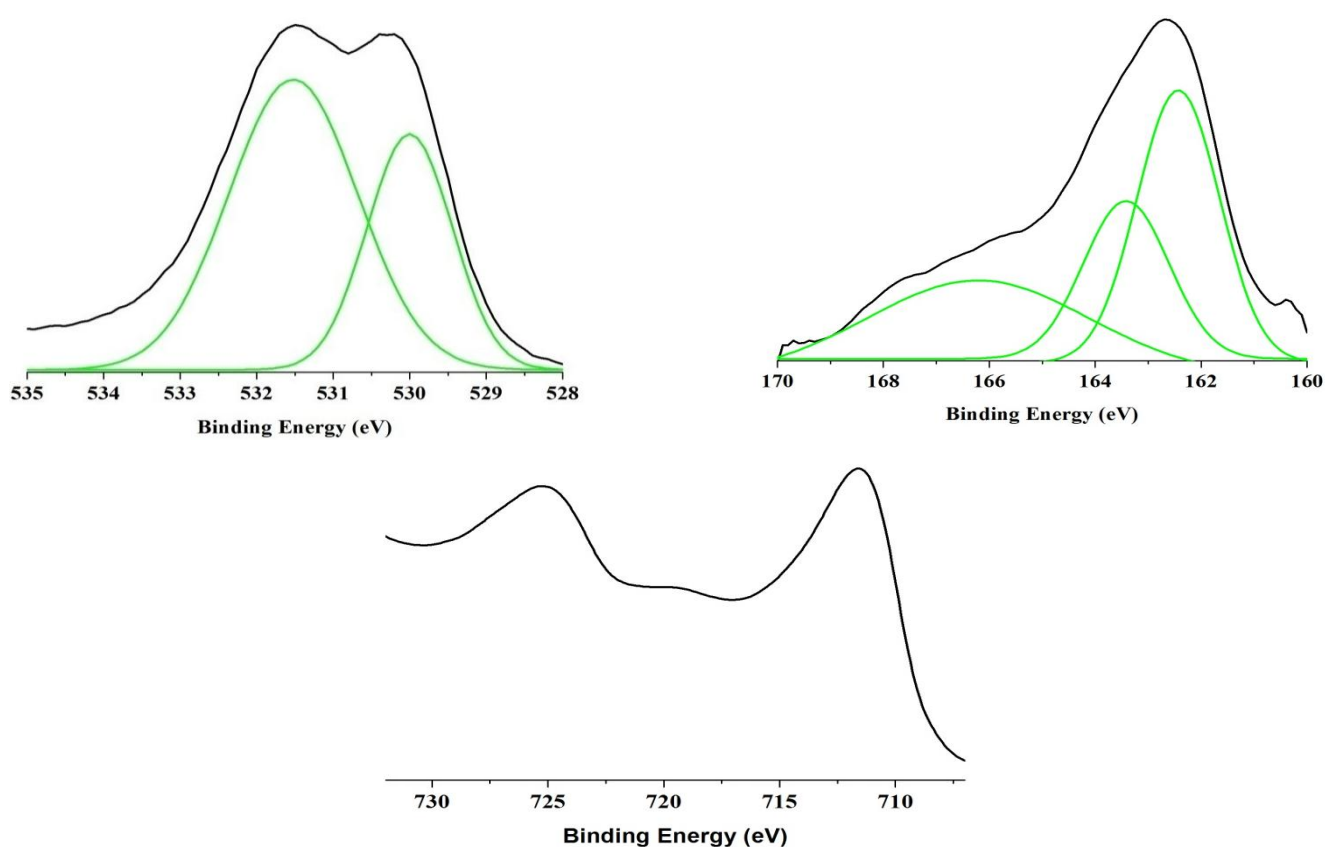


Figure 6: HCS spectra of a) O2s, b) S2p c) Fe2p, in presence of 100ppm concentrations of inhibitor C1

3.5 UV-Visible and IR spectroscopy

UV-Visible spectra were recorded on the samples after the experiments were done and the surface was scrapped and dissolved in DMSO. The spectra show a new band at 580 nm in additions to those bands which are discussed earlier. The original peaks of the inhibitors undergo a hypsochromic shift because of surface coordination. The band at 580 nm is typical of d-d transitions observed in the Fe (III) complexes. It clearly indicates the formation of chemisorbed films of the inhibitor on the HCS surface. The FTIR spectra of the scrapped samples of the both high carbon steel show the shifting on their stretching frequency of the inhibitor reveal that the inhibitor coordinate to the surface of the metal active site. The broad band at 3100-3400 assigned to the stretching frequency of the water, NH stretching band disappears of C=N at 1618 (C1) and 1628 (C2), C-S stretching band at 1378 (C1) and 1383 (C2) due to the Metal and (C1&C2) complex. The shifting of IR value clearly indicates those inhibitors was absorbed on the metal surface and protect the corrosion from the acid.

Table 5: XPS for the metal absence and presence of C2.

Substrate	High Carbon steel		HCS with inhibitor	
	BE/eV	Assignment	BE/eV	Assignment
C1s	285.1	-C-,	284.75	-C-,
			285.35	
			286.15	-CH ₃
			288.45	C-N
N1s			398.95	C-N
			400.15	N-N
			400.85	N=N
O2s			530.0	FeO
			531.6	FeOOH
S2p			162.4	Fe _{1-x} S
			163.4	-S-
			166.2	S ₆
			711.65	FeO, FeS
Fe2p	710.4	FeO	719.95	
			724.5	FeOOH Fe ₂ O ₃ , Fe ₃ O ₄
			725.65	FeOOH, Fe ₂ O ₃ , Fe ₃ O ₄

3.6 Adsorption isotherm

From the spectral data, there is a definitive chemisorption on the surface to protect against the corrosion of high carbon steel by adsorption on the metal-solution interface. C1&C2 has adsorbed on the active corrosion site of the metal and diminish the corrosion from the acid. The reactive functional groups present in the C1&C2 leads to the chemisorption process. The surface coverage (θ) for different concentrations of (C1 and C2) in acidic media has been evaluated from impedance measurements and Tafel by using the following equation [44]:

Fig.7 (a, b) Shows the plot of C_{inh}/θ vs. C_{inh} yielded the straight line. The linear correlation coefficient (r^2) is almost equal to 1 ($r^2 = 0.99$) and the slope is very close to 1, indicating the adsorption of synthesized (C1&C2) on the metal surface obeys the Langmuir adsorption isotherm. The equilibrium constant (K_{ads}) for the adsorption of (C1&C2) was calculated from the reciprocal of the intercept straight line. The free energy of the absorption was calculated from the following equation:

$$\Delta G_{ads} = -RT \ln K_{ads}$$

Calculated free energy and equilibrium constant is given in Table 5. The spontaneity and stability of the adsorption on the HCS surface of inhibitor occurred from the negative value of the free energy. The free energy values indicate a strong adsorption of the synthesized (C1&C2) on the surface of carbon steel in 1.0 M HCl. According to Noor [45], ΔG_{ads} values in between -20 to -40 kJ mol⁻¹ mixed type of inhibitors (chemisorption and physisorption). For our investigation C1 ΔG_{ads} value -33.81 (EIS) and -34.79 (Tafel), C2 ΔG_{ads} value -34.30 (EIS) and -36.41 (Tafel). ΔG_{ads} values indicate that the (C1&C2) were mixed type inhibitor both chemisorption (electrostatic) and physisorption (charge transfer) and their value were in between -20 to -40 kJ mol⁻¹.

Table 8: Langmuir adsorption isotherm for HCS immersed in 1.0 M HCl solution in presence of C1-C2

Metal	Methods	R ²	Slope	ΔG_{ads} (kJ/mol)	K_{ads} (kJ/mol)
C1	EIS	0.9986	1.0100	-33.81	13897
	Tafel	0.9987	1.0196	-34.79	20593
C2	EIS	0.9990	1.0142	-34.30	16915
	Tafel	0.9998	1.0009	-36.41	39525

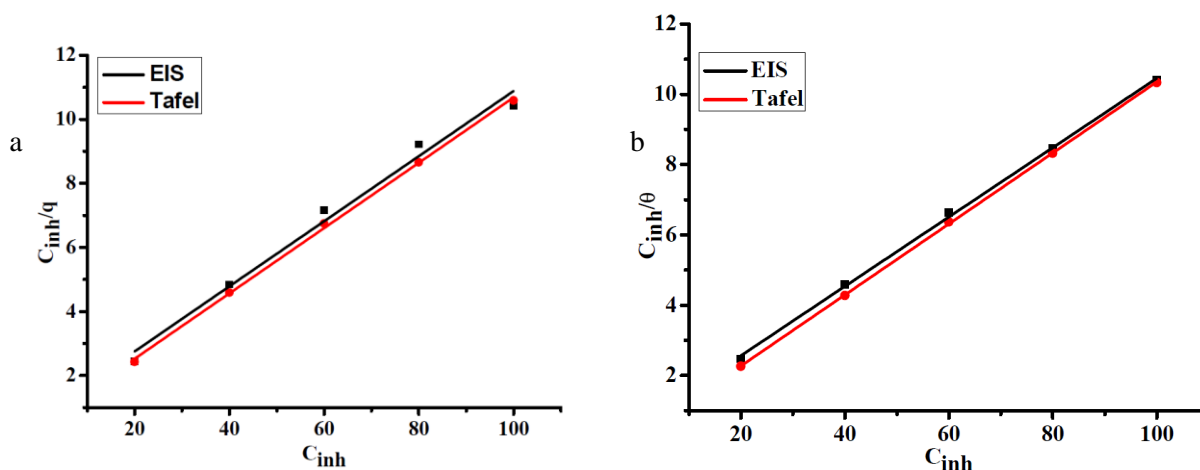


Fig.7 (a, b) : Plots of C_{inh}/θ vs. C_{inh}

3.7 Mechanism of inhibition

The inhibitors, EIS results clearly indicating the increased R_{ct} and decreased C_{dl} respectively, suggested that inhibitor species function by adsorption at the metal/solution interface. The adsorption may be possible in three ways: first one, charge transfer interaction of lone pair of electron in N, S or π electrons of the aromatic ring with vacant d orbitals of the Fe (chemisorption at anodic site), second electrostatic interaction between aromatic ring with Fe surface (physisorption at cathodic site), third was combination of both. According to Noor [45], ΔG_{ads} value was less than -20 kJ mol^{-1} it leads to physisorption, more than -40 kJ mol^{-1} chemisorption. In our study ΔG_{ads} value of the C1, C2 were around -34 to -36 kJ mol^{-1} . ΔG_{ads} value suggested that adsorption of piperazine dithiosemicarbazone on the high carbon steel surface arisen by both charge transfer (C=S, -NH) and electrostatic interaction (π electrons of the aromatic ring). Bis (Benzoyl pyridine) piperazine dithiosemicarbazone has been better inhibitive properties due to course of extra aromatic ring compared with Bis (pyridine-2-carboxaldehyde) piperazine dithiosemicarbazone.

Conclusions

Bis (Benzoyl pyridine) piperazine dithiosemicarbazone (C2) have been good inhibition efficiency compared to Bis (pyridine-2-carboxaldehyde) piperazine dithiosemicarbazone (C1), on the corrosion of mild steel in 1M HCl medium. Electrochemical studies EIS and polarization result reveals that the inhibition efficiency of the inhibitor increases with increasing concentration in high carbon steel. XPS surface analysis shows characterize passive film formed on the mild steel upon immersion in the acid. The adsorption of C1 and C2 in 1M HCl on the surface of high carbon steel obeys the Langmuir adsorption isotherm.

References

1. H. Lgaz, R. Salghi, S. Jodeh, B. Hammouti, *J. Mol. Liq.* 225 (2017) 271-280.
2. C. Kustu, C. Kaan, Emregul, O. Atakol, *Corros. Sci.* 49 (2007) 2800-2811.
3. A. Doner, R. Solmaz, M. Ozcan, G. Kardas, *Corros. Sci.* 53 (2011) 2902-2913.
4. A. Samide, B. Tutunaru, C. Negrila, *Chem. Biochem. Eng. Q.* 25 (2011) 299-308.
5. J.K. Swearingen, D. X. West, *Transition Metal Chemistry.* 25 (2000) 241-246.
6. R. Chandra, O. P. Pandey, S. K. Sengupta, *J. Agric. Food Chem.* 53 (2005) 2181-2184.
7. R. Tamilarasan, A. Sreekanth, *RSC Adv.* 3 (2013) 23681-23691.
8. E.E. Oguzie, *Mater Lett.* 59 (2005) 1076-1079.
9. M.A. Quraishi, I. Ahmad, A.K. Singh, *Mater Chem Phys.* 112 (2008) 1035-1042.
10. N.A. Negm, M.F. Zaki, *J. Surf Deterg.* 12 (2009) 321-329.
11. K.S. Jacob, G. Parameswaran, *Corros. Sci.* 52 (2010) 224-228.
12. R. Solmaz, *Corros. Sci.* 52 (2010) 3321-3330.
13. S. Xianghong, S. Deng, H. Fu, *Corros. Sci.* 53 (2011) 1529-15.
14. S. Safak, B. Duran, A. Yurt, G. Turkoglu, *Corros. Sci.* 54 (2012) 251-259.
15. B.V. Crist, *XPS Reports.* 1 (2007) 1-52.
16. A.A. Refaie, J. Walton, R.A. Cottis, R. Lindsay, *Corros. Sci.* 52 (2010) 422-428.
17. G. Gece, *Corros. Sci.* 50 (2008) 2981-2992.

18. S. DemetOzkır, K. Kayakırılmaz, E. Bayol, A.A. Gurten, F. Kandemirli, *Corros. Sci.* 56 (2010) 143–152.
19. H.A. Sorkhabi, N.G. Jeddi, F. Hashemzadeh, H. Jahani, *Electrochimica Acta.* 50 (2006) 3848-3854.
20. L. Elkadi, B. Mernari, M. Traisnel, F. Bentiss, M. Lagrenee, *Corros. Sci.* 42 (2000) 703-710.
21. M.A. Hegazy, A.M. Badawi, S.S. Abd El Rehim, W.M. Kamel, *Corros. Sci.* 56 (2012) 143–88.
22. S.S. Rahim, H.H. Hassan, M. A. Amin, *Mater. Chem. Phys.* 70 (2001) 64–72.
23. A. Yurt, S. Ulutas , H. Dal, *Appl. Surf. Sci.* 253 (2006) 919–925.
24. M.J. RodriguezPresa, R.I. Tucceri, M.I. Florit, D. Posadas, *J. Electroanal. Chem.* 475 (1999) 152.
25. B.D. Mert, M.E. Mert, G. Kardas, B. Yaz, *Corros. Sci.* 53 (2011) 4265–4272.
26. M. Abdallah, I. Zaafrany, S.O. Al-Karane, A.A. Abd El-Fattah, *Arabian Journal of Chemistry*, 5 (2012) 225–234
27. M.S. Morad, *Corros. Sci.* 42 (2000) 1307–1315.
28. Aljourani, J. Raeissi, K. Golozar, *Corros. Sci.* 51 (2009) 1836–1843.
29. S. H. AshassiSorkhabi, B. Shabani, B. Aligholipour, D. Seifzadeh, *Appl. Surf. Sci.* 252 (2006) 4039–4047.
30. M. O. Watanabe, S. Itoh, K. Mizushima, T. Sasaki, *Appl. Phys. Lett.* 68 (1986) 2962–2964.
31. P. Galicia, N. Batina, I. Gonzalez, *J. Phys. Chem. B* 110 (2006) 14398-14405.
32. S. Feliu Jr, V. Barranco, *Acta Materialia* 51 (2003) 5413–5424.
33. F. Bentiss, M. Traisnel, L. Gengembre, M. Lagrene, *Appl. Surf. Sci.* 152 (1999) 237–24.
34. V. S. Sastri, M. Elboujdaini, J. R. Brown, *Corros. Sci.* 52 (1996) 447-452.
35. T. Reier, S. Simson, J. W. Schultze, *Electrochimica Acta* 43 (1998) 149-148.
36. S. N.S. McIntyre, D.C. Zetaruk, *Anal. Chem.* 49 (1977) 1521.
37. C.R. Brundle, T.J. Chuang, K. Wandelt, *Surf. Sci.* 68 (1977) 459.
38. H. Abdel-Samad, P. R. Watson, *Appl. Surf. Sci.* 136 (1998) 46–54.
39. L. Forget, F. Wilwers, J. Delhalle, Z. Mekhalif, *Appl. Surf. Sci.* 205 (2003) 44–45.
40. D.D. Hawn, B.M. DeKoven, *Surf. Interface Anal.* 10 (1987) 63.
41. M. Muhler, R. Schlögl, G. Ertl, *J. Catal.* 138 (1992) 413.
42. C.D. Wagner, L.H. Gale, R.H. Raymond, *Anal. Chem.* 51 (1979) 466.
43. T. Yamashita, P. Hayes, *Appl. Surf. Sci.* 254 (2008) 2441–2449.
44. P. Velasquez, J.R. Barrado, R. Cordova, *Surf. Interface Anal.* 30 (2000) 149-153.
45. E.A. Noor, *Int. J. Electrochem. Sci.* 2 (2007) 996.
46. M. El Faydy, T. Djassinra, S. Haida, M. Rbaa, K. Ounine, A. Kribii, B. Lakhrissi, *J. Mater. Environ. Sci.* 8 (2017) 3855-3863.
47. L. El Ouasif, I. Merini, H. Zarrok, M. El ghou, R. Achour, A. Guenbour, H. Oudda, F. El-Hajjaji, B. Hammouti, *J. Mater. Environ. Sci.* 7 (8) (2016) 2718-2730.

(2018) ; <http://www.jmaterenvirosci.com>